The Astrophysical Journal, 657: L89–L92, 2007 March 10

THE HERCULES-AQUILA CLOUD

V. Belokurov,[1] N. W. Evans,[1] E. F. Bell,[2] M. J. Irwin,[1] P. C. Hewett,[1] S. Koposov,[2] C. M. Rockosi,[3] G. Gilmore,[1] D. B. Zucker,[1] M. Fellhauer,[1] M. I. Wilkinson,[1] D. M. Bramich,[1] S. Vidrih,[1] H.-W. Rix,[2] T. C. Beers,[4] D. P. Schneider,[5] J. C. Barentine,[6] H. Brewington,[6] J. Brinkmann,[6] M. Harvanek,[6] J. Krzesinski,[6] D. Long,[6] K. Pan,[6] S. A. Snedden,[6] O. Malanushenko,[6] and V. Malanushenko[6]

Received 2006 December 12; accepted 2007 January 25; published 2007 February 12

ABSTRACT

We present evidence for a substantial overdensity of stars in the direction of the constellations of Hercules and Aquila. The cloud is centered at a Galactic longitude of $l \approx 40°$ and extends above and below the Galactic plane by at least 50°. Given its off-centeredness and height, it is unlikely that the Hercules-Aquila cloud is related to the bulge or thick disk. More likely, this is a new structural component of the Galaxy that passes through the disk. The cloud stretches ~80° in longitude. Its heliocentric distance lies between 10 and 20 kpc so that the extent of the cloud in projection is ~20 kpc by ~15 kpc. It has an absolute magnitude of $M_v = -13$, and its stellar population appears to be comparable to, but somewhat more metal-rich than, M92.

Subject headings: galaxies: kinematics and dynamics — galaxies: structure — Galaxy: halo — Local Group

1. INTRODUCTION

The construction of the Milky Way via the hierarchical aggregation of small galaxies has left behind debris in the form of streams, satellites, and substructure in the Galactic halo. There are many examples now known of such detritus, including the disrupting Sagittarius galaxy and its stream (e.g., Ibata et al. 2001; Majewski et al. 2003; Belokurov et al. 2006), the Monoceros Ring (e.g., Yanny et al. 2003), and the Orphan stream (e.g., Belokurov et al. 2007). In addition to the easily recognizable streams, the depth and wide area coverage of the Sloan Digital Sky Survey (SDSS) enables identification of other less well defined features. A substantial overdensity in the direction of Virgo (Juric et al. 2006) and a possible underdensity in the direction of Ursa Major (Xu et al. 2006) have been found. Here we identify and characterize another overdensity of stars, called the *Hercules-Aquila cloud*.

2. THE HERCULES-AQUILA CLOUD

SDSS imaging data are produced in five photometric bands, namely, *u*, *g*, *r*, *i*, and *z* (see, e.g., Fukugita et al. 1996; Hogg et al. 2001; Smith et al. 2002; Gunn et al. 2006), and are automatically processed through pipelines to measure photometric and astrometric properties and to select targets for spectroscopic follow-up (Lupton et al. 1999; Stoughton et al. 2002; Pier et al. 2003; Ivezić et al. 2004). In this Letter, all the photometric data are dereddened using the maps of Schlegel et al. (1998). We use primarily Data Release 5 (DR5), which covers ~8000 deg^2 around the Galactic north pole, and three stripes in the Galactic southern hemisphere (Adelman-McCarthy et al. 2007). While the motivation for the original SDSS was largely extragalactic, a substantial portion of its successor survey SDSS II is devoted to Galactic structure (the Sloan Extension for Galactic Understanding and Exploration [SEGUE]). There are a number of SEGUE imaging stripes that run from positive to negative latitudes through the disk at constant longitude.

Figure 1 shows an RGB composite density map of stars with $20 < i < 22.5$ and $0.1 < g - i < 0.7$ in Galactic coordinates centered at ($l = 0°$, $b = 0°$). As illustrated in the inset, blue represents the density of stars with $0.1 \le g - i < 0.3$, green those with $0.3 \le g - i < 0.5$, and red those with $0.5 \le g - i < 0.7$. A number of the prominent substructures that dominate the halo are marked, including the Sagittarius stream, the Monoceros Ring, the Virgo overdensity, and the Orphan stream. The subject of this Letter is the gold-colored overdensity that is most prominent in DR5 at longitudes of ~40° and is visible in both hemispheres. This is the Hercules-Aquila cloud. Overlaid on the plot are contours of constant total extinction from Schlegel et al. (1998).

To investigate this structure, we exploit the SEGUE imaging at $l = 31°$ (runs 5378 and 5421) and 50° (run 4828), shown as the two red dashed lines in Figure 1. Each SDSS and SDSS II stripe comprises two interlocking runs, each of which has a width of 2.34° but covers half the area of the stripe. In Figure 2, we show the density of stars in the runs with $0.25 < g - i < 0.4$ in units of mag^{-1} deg^{-2}. The color cut is designed to identify primarily halo stars. We also show profiles of density and extinction as well as their differences (in red, green, and blue lines, respectively). We see that, comparing the northern and southern hemispheres, there is dramatic asymmetry at $l = 50°$ with a substantial overdensity at negative latitudes. The asymmetry is still present at $l = 31°$, but the overdensity now occurs at positive latitudes.

The structure is seen most cleanly in the difference maps in the bottom two panels of Figure 2. Here overdensities relative to the other hemisphere are dark, while underdensities are white. The Hercules-Aquila cloud is seen clearly at $l = 31°$, $b \approx 20°$, $i \approx 19$ mag and $l = 50°$, $b \approx -15°$, $i \approx 20$ mag. It is therefore closer to the Sun at $l = 31°$ than at $l = 50°$. There are two further overdensities visible in Figure 2 at $l = 31°$,

[1] Institute of Astronomy, University of Cambridge, Cambridge, UK; vasily@ast.cam.ac.uk, nwe@ast.cam.ac.uk.
[2] Max Planck Institute for Astronomy, Heidelberg, Germany.
[3] Lick Observatory, University of California, Santa Cruz, CA.
[4] Department of Physics and Astronomy, Center for the Study of Cosmic Evolution, and Joint Institute for Nuclear Astrophysics, Michigan State University, East Lansing, MI.
[5] Department of Astronomy and Astrophysics, Pennsylvania State University, University Park, PA.
[6] Apache Point Observatory, Sunspot, NM.

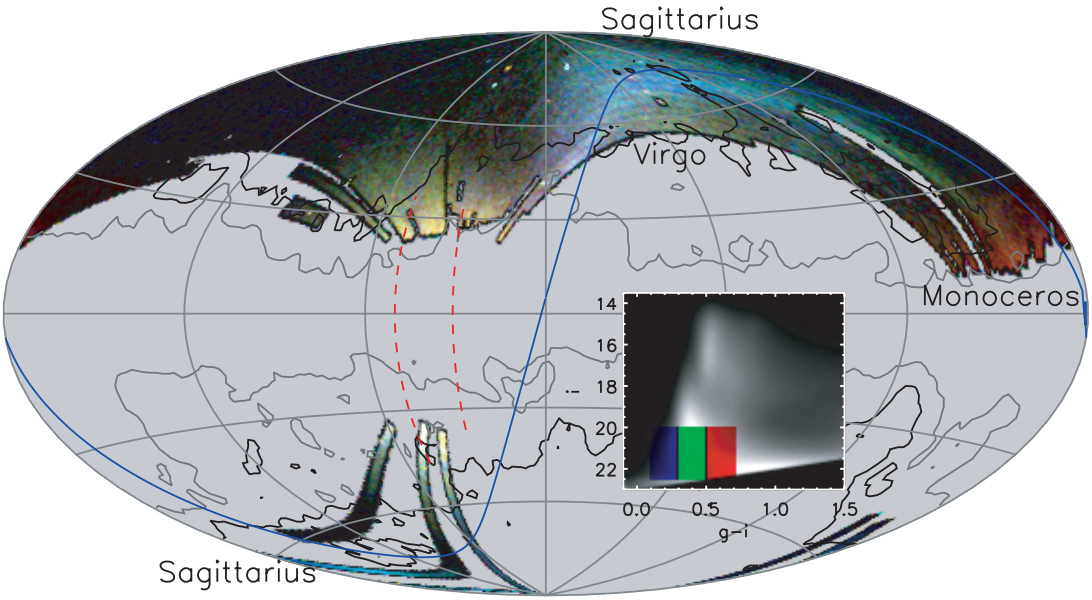

FIG. 1.—Areal density of SDSS stars with $0.1 < g - i < 0.7$ and $20 < i < 22.5$ in Galactic coordinates. The color plot is an RGB composite with blue representing $0.1 \le g - i < 0.3$, green $0.3 \le g - i < 0.5$, and red $0.5 \le g - i < 0.7$. Structures visible on the figure include the arch of the Sagittarius stream and the Orphan stream in blue and the multiple wraps of the Monoceros Ring in red. Behind, and offset from, the Galactic bulge, there is a yellow-colored structure visible in SDSS data in both hemispheres, centered at $l \approx 40°$. This is the Hercules-Aquila cloud. Overlaid on the plot are contours of constant extinction (black is 0.1 mag and gray is 0.25 mag in the i band). The two red vertical lines show the SEGUE stripes at $l = 31°$ (runs 5378 and 5421) and 50° (run 4828). The inset is a CMD of the SDSS data, with blue, green, and red bands encompassing the stars used to create the large figure.

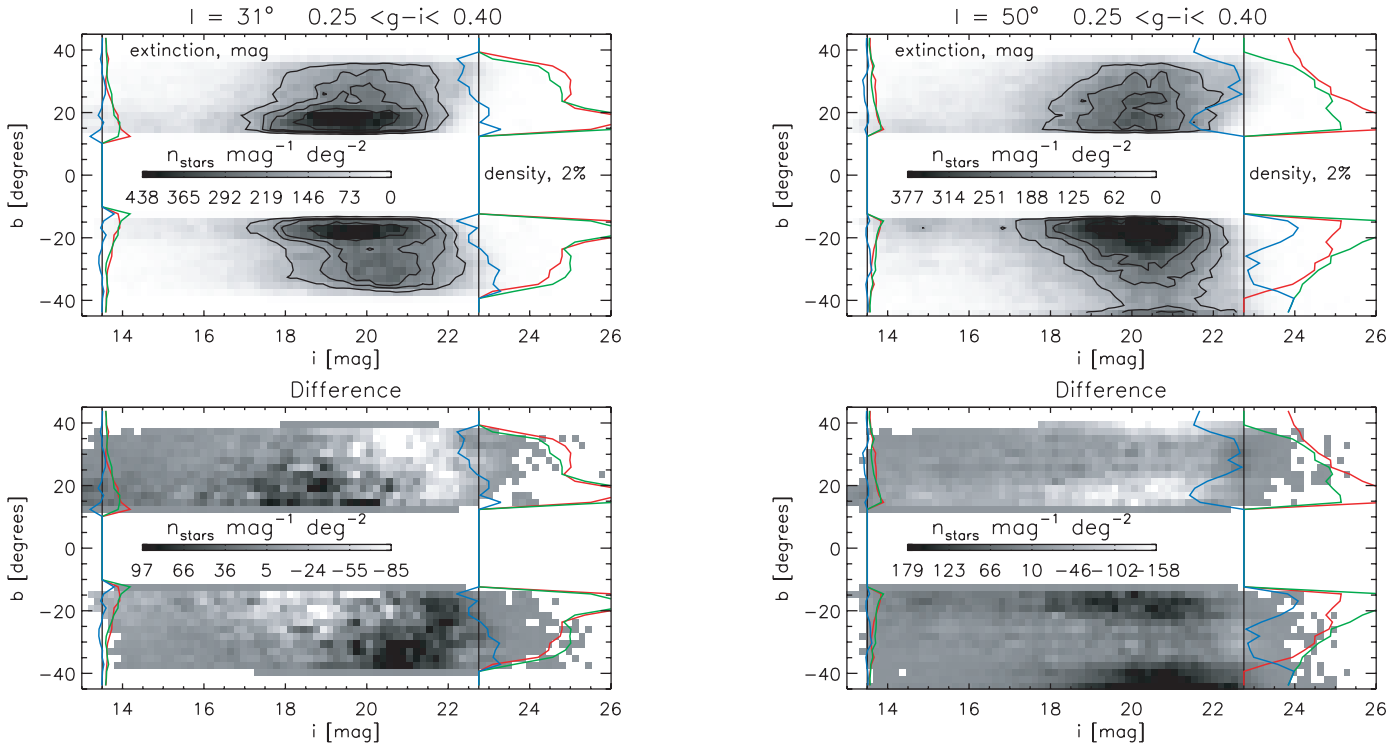

FIG. 2.—*Top panels*: Gray-scale contours of the spatial density of SDSS stars with $0.25 < g - i < 0.4$ in two slices at longitude $l = 31°$ (*left*) and $l = 50°$ (*right*). The spatial density is measured in mag^{-1} deg^{-2}. In each case, the leftmost (rightmost) colored lines shows the variation of extinction (density) with latitude in each hemisphere. Green denotes the current profile, while red refers to the opposite hemisphere and blue the difference. There are a number of prominent enhancements of density along the line of sight, as manifested by green profiles, which are not smoothly decaying curves but show bumps. The southernmost overdensities are associated with the Sagittarius stream ($l = 31°$, $b \approx -35°$, $i \approx 20.5$ mag and $l = 50°$, $b \approx -40°$, $i \approx 20.5$ mag). The other enhancement is part of the Hercules-Aquila cloud, which is revealed in the difference plots shown in the bottom panels. These are created by subtracting the density in the two hemispheres so that black (white) indicates relative overdensity (underdensity). The Hercules-Aquila cloud is at $l = 31°$, $b \approx 20°$, $i \approx 19.0$ mag and $l = 50°$, $b \approx -15°$, $i \approx 20.0$ mag.

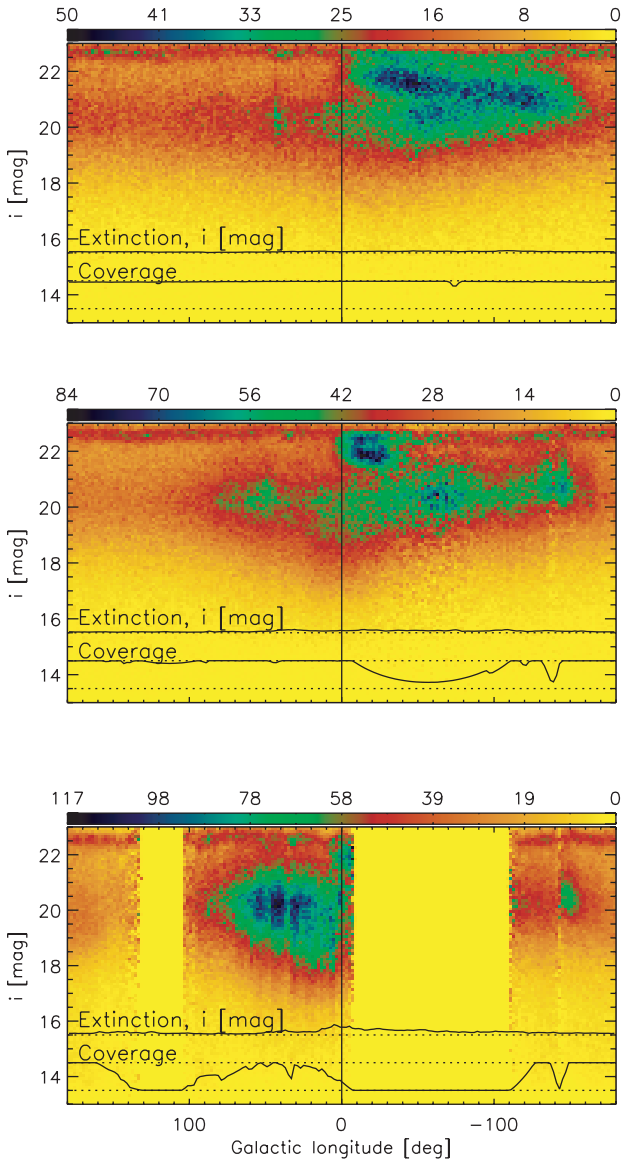

FIG. 3.—Three density slices at $b = 70°$ (*top*), 55° (*middle*), and 40° (*bottom*), each of which is 15° wide. The key gives the scale in number of stars mag^{-1} deg^{-2} satisfying the color cut $0.25 < g - i < 0.4$. The variation of the extinction along the strips and the fraction (between 0 and 1) covered in DR5 are shown as a function of longitude at the bottom of the panels. Three structures are discernible in the panels, and they are clearly separated. In the top panel, the Sagittarius stream and Virgo overdensity are seen to cross each other obliquely, while the tip of the Hercules-Aquila cloud is just visible; in the middle panel, the Sagittarius stream is bifurcated and cleanly differentiated from the Virgo overdensity, while the Hercules-Aquila cloud is becoming more substantial; in the bottom panel, only the Hercules-Aquila cloud is seen, due to SDSS DR5 coverage.

$b \approx -35°$, $i \approx 20.5$ mag and $l = 50°$, $b \approx -40°$, $i \approx 20.5$ mag. They are most likely associated with the Sagittarius stream. The orbital plane of the Sagittarius dwarf spheroidal galaxy as computed in Fellhauer et al. (2006) is shown as a blue dotted line in Figure 1. Its tidal debris has a thickness of ~15° on the sky and so should intersect the SEGUE imaging runs at their southernmost latitudinal points.

In the slice at $l = 50°$, the total number of excess stars with the color cut $0.25 < g - i < 0.4$, the latitude cut $-35° < b < 0°$, and within the contour corresponding to $n_{\rm stars} = 50$ in the bottom right panel of Figure 2 is 10^4. This ignores the contribution above the plane and so is a conservative estimate. Scaling to the overall longitudinal extent of the cloud, we estimate that there are 5×10^5 stars with $0.25 < g - i < 0.4$. Comparing with the color-magnitude diagram (CMD) of the metal-poor globular cluster M92, we estimate an absolute magnitude of $M_v = -13$ for the overdensity.

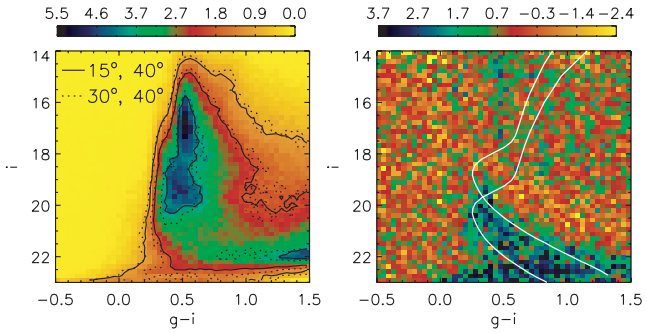

FIG. 4.—*Left*: Hess diagrams for the on-cloud field at $l = 30°$, $b = 40°$ (*dotted lines*) and the off-cloud field at $l = 15°$, $b = 40°$ (*solid lines*). The units are 10^4 stars mag^{-2}. *Right*: Difference of the Hess diagrams divided by the square root of their sum. This shows essentially the signal-to-noise ratio in the difference. There is one obvious overdensity corresponding to upper main sequence and turnoff stars in the Hercules-Aquila cloud. The white lines show M92 ridgelines shifted to the distance of 10 and 20 kpc, which bracket the main-sequence location.

Figure 3 shows longitudinal cuts through the Hercules-Aquila cloud at three latitudes: $b = 70°$, 55°, and 40°, each 15° wide. The SDSS data sometimes only partly cover the slice. To take this incompleteness into account, we normalize the density in each longitude bin by the fraction covered. There are three structures visible in the panels. The bifurcated Sagittarius stream and the Virgo overdensity dominate the top two panels. However, in both panels, a new structure is becoming visible; this is the Hercules-Aquila cloud. In the bottom panel, the cloud has come clearly into view, extending over 90° in longitude, while the Sagittarius and the Virgo overdensity are largely missing in the area covered by the DR5 footprint.

Figure 4 shows Hess diagrams for a 8° × 8° field centered on $l = 30°$, $b = 40°$, and a 16° × 16° field centered on $l = 15°$, $b = 40°$ (*left*), together with their difference divided by the square root of their sum (*right*). The two fields are chosen to lie interior to and exterior to the cloud at the same latitude. In the difference panel, there is a clear upper main sequence and turnoff, corresponding to stars in the cloud. Also shown in white are two M92 ridgelines, using data from Clem (2005) that are used to bracket the distance range in the Hercules-Aquila cloud. These suggest that the cloud in SDSS DR5 is primarily composed of upper main sequence and turnoff stars at heliocentric distances of between 10 and 20 kpc. The turnoff lies redward of the M92 ridgeline, suggesting that the cloud is composed of more metal-rich stars than M92 ([Fe/H] = −2.2).

Figure 5 shows the kinematic evidence for the Hercules-Aquila cloud using SDSS radial velocities for stars with $g - r < 1$ and $r < 19$. All the velocities are converted to the Galactic standard of rest and have a typical uncertainty of ~10 km s^{-1}. The first field covers the cloud ($20° \le b \le 55°$ and $20° \le l \le 75°$). There are two comparison fields at larger longitude and higher latitude, namely, field 2 at $40° \le b \le 55°$ and $110° \le l \le 180°$, and field 3 at $65° \le b \le 80°$ and $20° \le l \le 80°$. Most of the stars are at high latitude and selected to be bluer than the thin-disk dwarfs. The signal is therefore dominated by halo and thick-disk stars. This is clear from the thick gray histogram in Figure 5, which reports velocities for all stars in field 1. The

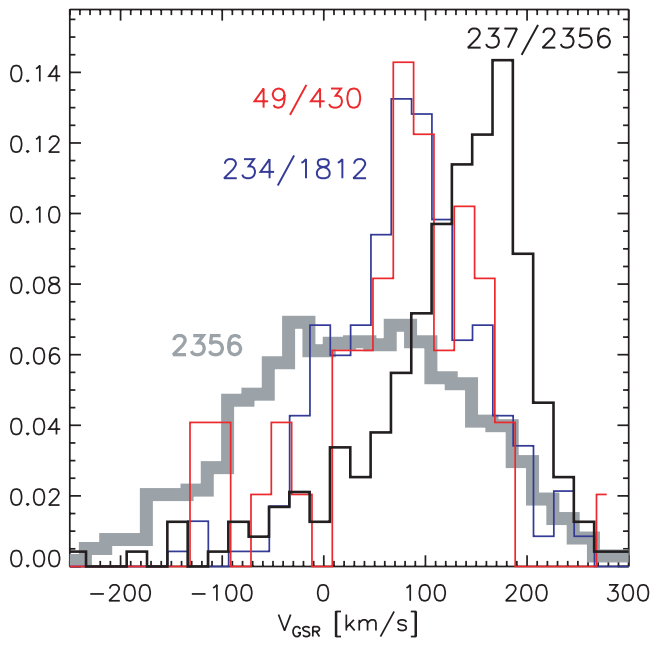

FIG. 5.—Histograms of velocities (converted to the Galactic standard of rest) for stars with $g - r < 1$ and $r < 19$. Thick gray lines refer to all stars in the field centered on the Aquila-Hercules cloud. We select red giant branch candidates from the CMD in three fields, two off-cloud (*red and blue*) and one on-cloud (*black*). The red and blue histograms peak at ~80 km s^{-1}, as expected for thick-disk stars. The black histogram peaks at ~180 km s^{-1}, which we interpret as the velocity signature of the cloud. The total numbers of stars in the fields after the CMD cut, as well as those picked up by the CMD mask, are marked in color above the histograms.

distribution is built from one component with almost zero mean velocity and another with mean at ~80 km s^{-1}. The all-star velocity distribution is the same for fields 2 and 3 and not shown. To pick out the stars in the structure, we use a mask based on the M92 ridgeline, shifted to 10 and 20 kpc. The distribution for field 1 centered on the Hercules-Aquila cloud is shown as a black solid line and can be compared to the histograms for the off-cloud fields 2 and 3 (*blue and red, respectively*). Nearby thick-disk stars in these locations have a line-of-sight velocity of ~150 sin l cos b ~ 80 km s^{-1} with respect to the Galactic standard of rest (e.g., Gilmore et al. 1989), which is consistent with the peaks in the red and blue histograms. There is a clear kinematic signal from stars moving coherently with a radial velocity of ~180 km s^{-1} in the on-cloud field. This cannot be due to either the halo or the thick disk.

Could the Hercules-Aquila cloud be related to the Galactic bulge or bar? There is an asymmetry in the integrated light of the bulge, famously seen by the Diffuse Infrared Background Experiment instrument on the *Cosmic Background Explorer* satellite (Dwek et al. 1995), but it is only of the order of a few degrees at most (see, e.g., Weiland et al. 1994). This asymmetry would be larger if confined to stars in a range of heliocentric distances between 4 and 8 kpc, as we would then be primarily picking up stars on the near side of the bar. However, our estimate of the distance to the Hercules-Aquila cloud is 10–20 kpc. At $l = 40°$, the closest the cloud can be to the Galactic center is in the range 6–15 kpc. Although the cloud passes through the disk, it seemingly lies well beyond the Galactic bar. Also, the cloud extends to Galactic latitudes of $\pm 50°$, again much larger than the vertical scale height of the bulge or of the thin and thick disks. Parker et al. (2003, 2004) also discovered some asymmetries in the distribution of bright, probably thick-disk, stars using POSS I data, but these stars are much closer at ~2 kpc from the Sun.

Could the Hercules-Aquila cloud be a smooth component that is centered on $l = 0°$ but made to appear asymmetric by extinction? Most of the extinction is caused by dust with a scale length of ~100 pc. However, there is a prominent north polar spur of dust that extends to high Galactic latitudes (see, e.g., Frisch 1981). This can be seen in Figure 1 as the extension to the black contour over latitudes 30°–60°, where it overlaps part of the Sagittarius stream. However, a similar amount of extinction appears to have no effect on the underlying density of detected stars in the Sagittarius stream and the Virgo overdensity at $l = -100°$, and so variable extinction is not a plausible explanation of the offset structure. *We conclude that the Hercules-Aquila cloud is a real, hitherto unknown, structural component of the inner halo of the Galaxy.*

Funding for the SDSS and SDSS II has been provided by the Alfred P. Sloan Foundation, the Participating Institutions, the National Science Foundation, the US Department of Energy, the National Aeronautics and Space Administration, the Japanese Monbukagakusho, the Max Planck Society, and the Higher Education Funding Council for England. The SDSS Web site is http://www.sdss.org.

REFERENCES

Adelman-McCarthy, J. K., et al. 2007, ApJS, submitted
Belokurov, V., et al. 2006, ApJ, 642, L137
———. 2007, ApJ, in press
Clem, J. L. 2005, Ph.D. thesis, Univ. Victoria
Dwek, E., et al. 1995, ApJ, 445, 716
Fellhauer, M., et al. 2006, ApJ, 651, 167
Frisch, P. C. 1981, Nature, 293, 377
Fukugita, M., Ichikawa, T., Gunn, J. E., Doi, M., Shimasaku, K., & Schneider, D. P. 1996, AJ, 111, 1748
Gilmore, G., King, I., & van der Kruit, P. 1989, The Milky Way as a Galaxy (Geneva: Geneva Obs.)
Gunn, J. E., et al. 2006, AJ, 131, 2332
Hogg, D. W., Finkbeiner, D. P., Schlegel, D. J., & Gunn, J. E. 2001, AJ, 122, 2129
Ibata, R., Lewis, G. F., Irwin, M., Totten, E., & Quinn, T. 2001, ApJ, 551, 294
Ivezić, Ž., et al. 2004, Astron. Nachr., 325, 583
Juric, M., et al. 2006, ApJ, submitted (astro-ph/0510520)
Lupton, R., Gunn, J., & Szalay, A. 1999, AJ, 118, 1406
Majewski, S. R., Skrutskie, M. F., Weinberg, M. D., & Ostheimer, J. C. 2003, ApJ, 599, 1082
Parker, J. E., Humphreys, R. M., & Beers, T. C. 2004, AJ, 127, 1567
Parker, J. E., Humphreys, R. M., & Larsen, J. A. 2003, AJ, 126, 1346
Pier, J. R., Munn, J. A., Hindsley, R. B., Hennessy, G. S., Kent, S. M., Lupton, R. H., & Ivezić, Ž. 2003, AJ, 125, 1559
Schlegel, D., Finkbeiner, D., & Davis, M. 1998, ApJ, 500, 525
Smith, J. A., et al. 2002, AJ, 123, 2121
Stoughton, C., et al. 2002, AJ, 123, 485
Weiland, J. L., et al. 1994, ApJ, 425, L81
Xu, Y., Deng, L. C., & Hu, J. Y. 2006, MNRAS, 368, 1811
Yanny, B., et al. 2003, ApJ, 588, 824